Photofunctional Scope of Fluorescent Dithienylethene Conjugates with Aza-Heteroaromatic Cations

Jialei Chen-Wu, David B. Guzmán-Ríos, Patricia Remón, José A. González-Delgado, Antonio J. Martínez-Martínez, Francisco Nájera, Jesús F. Arteaga, and Uwe Pischel*

A series of dithienylethene (DTE) photoswitches with aza-heteroaromatic cationic moieties is synthesized. The switches are characterized regarding their photochemical and photophysical properties in acetonitrile and in water. The efficiency of the switching and the photostationary state composition depend on the degree of π-conjugation of the heteroaromatic systems. Thus, DTEs with acridinium-derived moieties have very low quantum yields for the ring-closing process, which is in contrast to switches with pyridinium and quinolinium moieties. All switches emit fluorescence in their open forms. The involved electronic transitions are traced back to an integrative picture including the DTE core and the cationic arms. The emission can be fine-tuned by the π-conjugation of the heteroaromatic cations, reaching the red spectral region for DTEs with acridinium moieties. On ring-closing of the DTEs the fluorescence is not observable anymore. Theoretical calculations point to rather low-lying energy levels of the highly conjugated ring-closed DTEs, which would originate near-infrared emission (> 1200 nm). The latter is predicted to be very weak due to the concurrent non-radiative deactivation, according to the energy-gap law. In essence, an ON–OFF fluorescence switching as the result of the electrocyclic ring-closing reaction is observed.

1. Introduction

Molecular systems that can be reversibly toggled by light between two or sometimes even more forms are known as photoswitches.[1–4] The photochemical conversion between these switch forms causes dramatic changes of the electronic and geometrical properties, which can be used for a plethora of applications, including for example information processing and storage,[5–13] photopharmacology,[14–16] light-gated catalysis,[17] light-induced delivery,[13,18–20] or imaging.[21–24] Among the most popular architectures the family of dithienylethenes (DTEs) can be found.[25–30] In their open form, these switches generally absorb light at shorter wavelengths (<400 nm). The conrotatory 6π-electrocyclization, commonly initiated by UV light, increases the degree of π-conjugation and leads to a colored ring-closed form.[28] When the latter is subjected to visible-light irradiation (usually >550 nm) the ring-open form is recovered.[28] The DTE switches can be operated in multiple ring closing/opening cycles with significant fatigue resistance.[28] The design of new DTE photoswitches has focused on several performance aspects, such as increased fatigue resistance,[23,24,31] negative photochromism,[32] all-visible-light photoswitching,[33] photoswitching induced by near-infrared light,[19,34] or multiphoton-induced switching.[35–38] Of specific interest is the development of fluorescent photoswitches with the possibility to switch the emission ON or OFF by a light stimulus.[28,39] This may be an advantage for imaging[23,24] and information processing applications.[28] As opposed to other diarylethenes,[40,41] or dithienylethenes with modified bridges,[42,43] the "original" DTEs with a (hexafluoro)cyclopentene bridge are generally known to be non-fluorescent or at best very weakly fluorescent.[28] However, chemical modification in form of sulfone DTE analogues yields fluorescent switches.[24,44,45] A different way to obtain fluorescent DTE switches is to combine them via non-conjugative linkers with fluorophores. The fluorescence of the latter depends on the switch form of the DTE, with the closed form enabling emission quenching via efficient energy transfer.[22,38,46–49] Very recently, a DTE derivative (not being an S-oxidized sulfone analogue) with a pyridinium and a quinolinium arm has been reported,

J. Chen-Wu, D. B. Guzmán-Ríos, P. Remón, J. A. González-Delgado,
A. J. Martínez-Martínez, J. F. Arteaga, U. Pischel
CIQSO-Centre for Research in Sustainable Chemistry and Department of Chemistry
University of Huelva
Campus de El Carmen s/n, Huelva E-21071, Spain
E-mail: uwe.pischel@diq.uhu.es
F. Nájera
Department of Organic Chemistry
University of Málaga
Campus Teatinos s/n, Málaga E-29071, Spain
F. Nájera
Instituto de Investigación Biomédica de Málaga y Plataforma en Nanomedicina-IBIMA
Plataforma Bionand
Parque Tecnológico de Andalucía, Málaga E-29590, Spain

The ORCID identification number(s) for the author(s) of this article can be found under https://doi.org/10.1002/adma.202300536
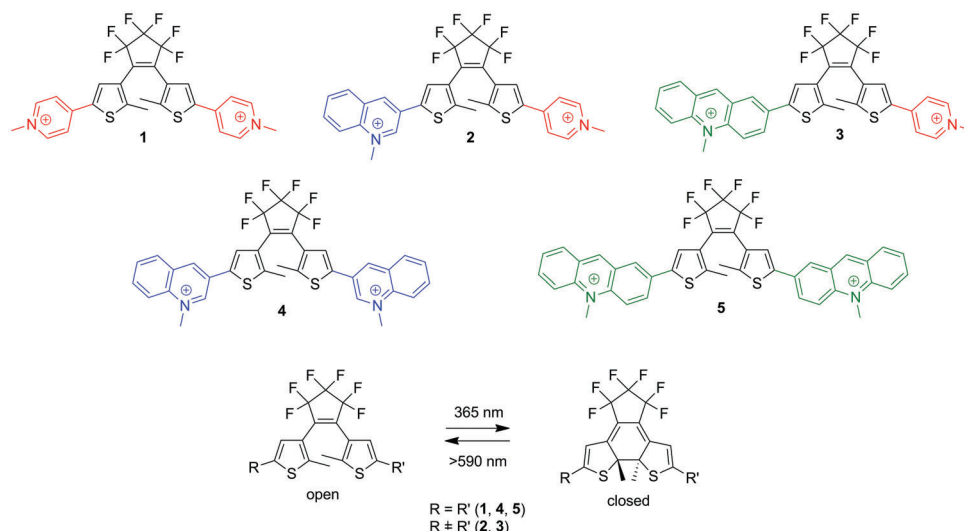
Figure 1. Structures of the DTE dyes **1–5** and general DTE photoswitching.

that shows fluorescence in the ring-open switch form.[50,51] The structure does not correspond to the DTE-fluorophore-conjugate format, but instead the branches are electronically entangled with the DTE core. In order to shine light on the origin of this rather uncommon finding, we expanded the scope of these potentially photoswitchable fluorophores. Thus, we synthesized a set of DTEs with heteroaromatic cationic branches, varying the substitution pattern (symmetric vs asymmetric DTEs) and degree of π-conjugation of the heteroaromatics; see structures **1–5** in **Figure 1**. The switches were subjected to a meticulous study of their photoswitching characteristics and fluorescence properties, as well as density-functional theory calculations. The fluorescence emission can be shifted into the red spectral region by using branches with higher π-conjugation, working even under application-relevant conditions, such as an aqueous environment.

2. Results and Discussion

2.1. Synthesis

The DTE photoswitches **1–5** were synthesized according to the synthetic routes shown in **Schemes 1** and **2**. A central building block was the bis-chlorinated compound DTE-Cl$_2$.[52] This was prepared from 2-methylthiophene via successive chlorination (with N-chlorosuccinimide) and bromination (with Br$_2$), followed by n-BuLi-mediated coupling to octafluorocyclopentene.[53] DTE-Cl$_2$ was subsequently used to access the accordingly substituted DTE compounds by means of Suzuki coupling reactions.[51] Finally, methylation of the heterocyclic aromatics (**1A**, **2A**, **3A–5A**) with methyliodide yielded the switches **1–5**. The compounds **1A** and **4A** were obtained by Suzuki coupling with commercially available pyridine-4-boronic acid or quinoline-3-boronic acid. For the preparation of non-symmetrically substituted **2A**, stepwise Suzuki coupling reactions starting from DTE-Cl$_2$ were performed, having **2B** as intermediary product.
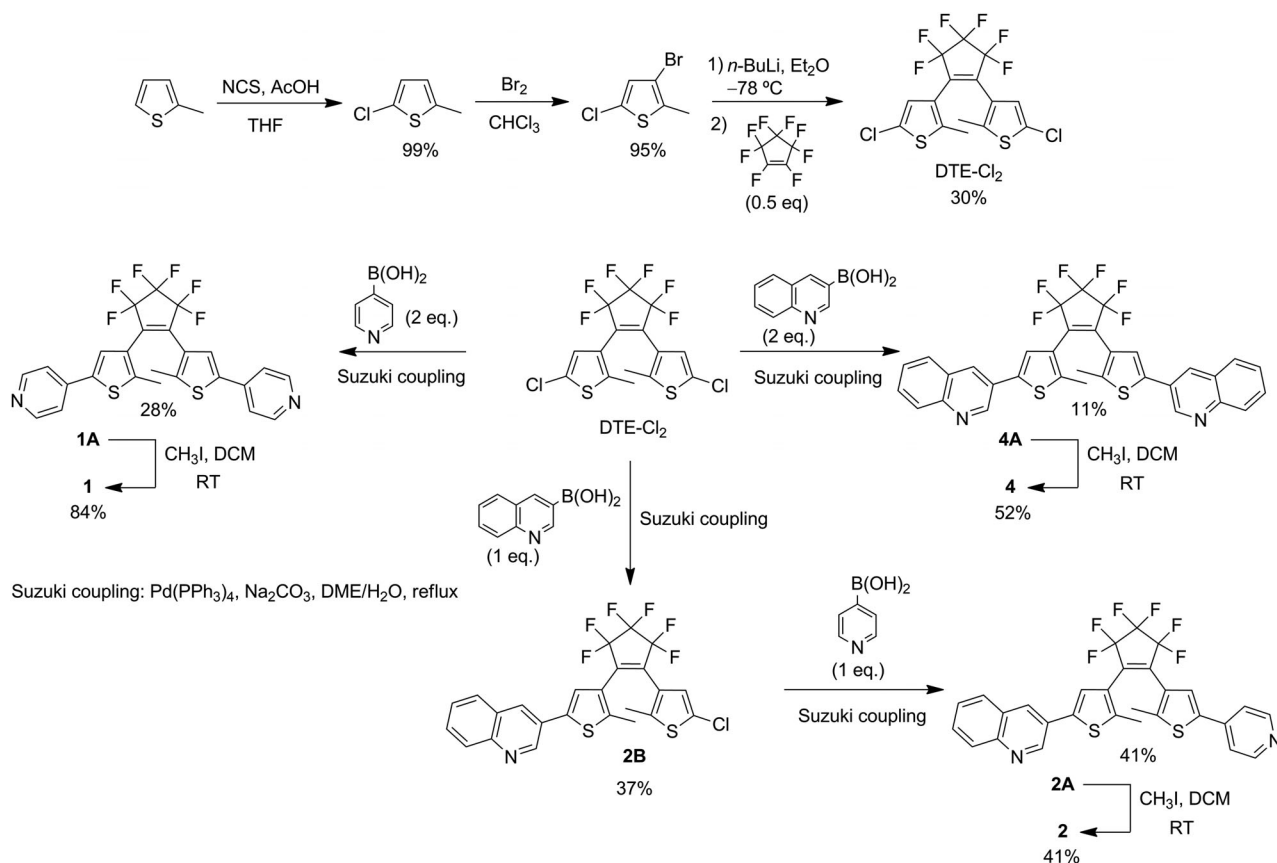
The acridine-substituted DTE switches **3** and **5** were obtained from DTE-Cl$_2$ by borylation[54] with B(i-PrO)$_3$ followed

by the Suzuki reaction with 2-iodoacridine and 4-bromopyridine (synthesis of **3A**) or 2-iodoacridine alone (synthesis of **5A**). 2-Iodoacridine was synthesized according to a published procedure by iodination of 9(10H)-acridanone with ICl, followed by reduction with BH$_3$ and oxidation with FeCl$_3$.[55] All relevant intermediary and final products were characterized by ^{1}H, ^{13}C, and ^{19}F NMR spectroscopy, gCOSY and gHSQC experiments, and high-resolution mass spectrometry (see the Supporting Information).

Crystals, suitable for single-crystal X-ray diffraction, were obtained for the open forms of the compounds **2** and **4**, the latter as modulated crystals. Both structures confirm the chemical integrity of the prepared switches (see **Figure 2**). Noteworthy, the crystal structure of **2** features the photochemically inactive parallel conformation. However, compound **4** crystallized in the photochemically active antiparallel conformation.[56] Coincidentally this goes against the observed trend for the ring-closing efficiency (0.54 vs 0.13 for **2** and **4**, respectively). However, the equilibrium situation between both conformers in solution is obviously different. On the NMR time scale the interchange between the parallel and antiparallel conformers is too fast in solution and only one set of signals was observed (see the Supporting Information). The packing of **2** in its crystal is governed by π–π stacking interactions between chemically identical cationic moieties, i.e., between pyridinium ions (3.3–3.6 Å interplane distance) or between quinolinium ions (3.1–3.2 Å interplane distance); see the Supporting Information. The symmetrically substituted switch **4** shows exclusively π–π stacking interactions between quinolinium branches (3.5 Å interplane distance). In this case, the highly ordered packing leads to a defined zig-zag arrangement; see the Supporting Information.

2.2. Photoswitching

The synthesized DTE derivatives **1–5** were first tested for their photoswitching performance in acetonitrile. The key data are summarized in **Table 1**. On excitation with 365-nm light, all DTE derivatives converted from their open forms (o) into the closed
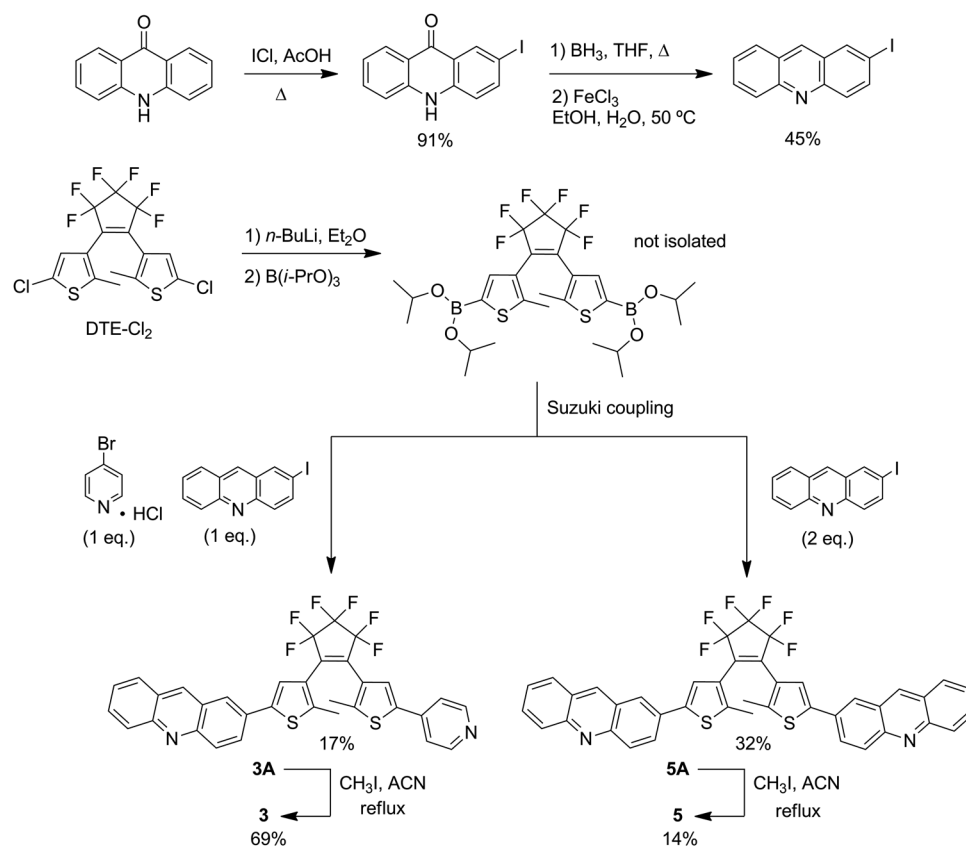
2300536 (2 of 11)

**ADVANCED
SCIENCE NEWS**

www.advancedsciencenews.com

**ADVANCED
MATERIALS**

www.advmat.de

Scheme 1. Preparation of the DTE dyes **1**, **2**, and **4**.

forms (c) by a 6π electrocyclization reaction. On the one hand, the closed forms, characterized by the appearance of a blue-colored solution, produced a spectrum with the characteristic long-wavelength band with a maximum at ca. 620–660 nm (see **Figure 3**). Irradiation of the closed form at wavelengths >590 nm regenerated the open form. These, on the other hand, are colorless (**1** and **2**), pale-yellow (**4**), or yellow colored (**3** and **5**), corresponding to the maximum of their longest wavelength absorption band (see Figure 3). In **Figure 4**, the temporal evolution of the absorption spectrum for the reversible transformation between the open and closed forms of DTE **3** is shown as an example (data for the other switches can be found in the Supporting Information). Either direction of isomerization, i.e., o→c or c→o, is characterized by multiple isosbestic points in the UV/vis absorption spectra. This hints on clean photochemical transformations without significant formation of secondary photoproducts.

The photostationary state distribution (PSD) on UV-light irradiation (365 nm) shows remarkable differences for the investigated switches. While **1** and **2** are converted quantitatively into their closed forms, the other three DTE switches show partial (78% and 85% closed form for **3** and **4**, respectively) or rather incomplete isomerizations (merely 44% closed form for DTE **5**). The different PSD are consistent with the measured quantum yields for the o→c and c→o transformations. DTE **1** features an extraordinarily high quantum yield for the o→c conversion ($\Phi_{o \to c} = 0.68$) in agreement with earlier published results for the same DTE in methanol.[57] The quantum yield for the ring open-

ing is far smaller ($\Phi_{c \to o} = 3 \times 10^{-3}$), giving rise to quantitative conversion on UV-light irradiation. Similar observations were made for DTE **2**. For the switches with partial o→c conversion (**3** and **4**) the quantum yields for the ring closing are significantly reduced (0.006 for **3** and 0.13 for **4**), but still higher than the reverse ring-opening process (≤ 0.002). Here, it is interesting to point out that even a rather inefficient o→c conversion for **3** is sufficient to yield ca. 80% ring closing in the photostationary state. Finally, for DTE **5**, ring-opening and closing have equally low quantum yields, and for this switch only ca. 44% of the open form is converted into the closed form. In all cases, the selective irradiation with visible light (>590 nm) yielded back the open forms in quantitative yield (100% open form).

The reason for the comparably quite inefficient ring-closing photoreaction of **3** and **5** may be sought in the occurrence of competitive excited-state processes. These switches contain one or two acridinium units, which are known as strong electron acceptors. Hence, concurrent intramolecular charge transfer (ICT) is a possible explanation for the observed reducing efficiency of the ring-closing process. The estimation of the driving force ($\Delta G_{ICT} = -0.81$ eV)[58] for the photoinduced oxidation of the ring-open DTE core by the acridinium electron acceptor leads to the conclusion that such process is indeed thermodynamically feasible. Further, the non-N-methylated analogue **3A** shows, in comparison, the usual high efficiency for the ring closing reaction ($\Phi_{o \to c} = 0.50$). This hints on the crucial role of the cationic nature in the observed effects.

**ADVANCED
SCIENCE NEWS**

www.advancedsciencenews.com

**ADVANCED
MATERIALS**

www.advmat.de

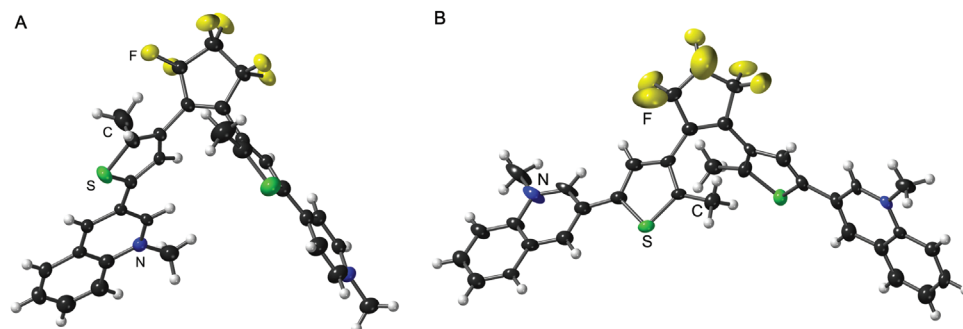**Scheme 2.** Preparation of the DTE dyes **3** and **5**.

Figure 2. A,B) Crystal structures of **2** (CCDC 2219894) (A) and **4** (CCDC 2219895) (B), showing displacement ellipsoids at 50% probability. Iodide ions and solvent molecules have been omitted for clarity.

In an effort to gain additional insight into the eventual interference of concurrent processes, the performance of the DTE switches on repeated closing/opening cycles was investigated. Especially the DTE dyes **1** and **2** showed good fatigue resistance (practically no degradation after five switching cycles and *ca.* 5% and 38% degradation for **1** and **2**, respectively, after 50 cycles); see **Figure 5** for **2** and the Supporting Information for **1**. The DTE switch **3** performed with good fatigue resistance over 5 cycles. However, upon prolonged switching (50 cycles), a notable fatigue (ca. 35%) and the build-up of absorption bands of secondary products was seen; see Figure 5. Finally, the DTEs **4** and **5** were characterized by more significant fatigue, leading to noticeable

decomposition (ca. 3–5%) already after five switching cycles. It is known that the introduction of additional methyl substituents at the thiophene rings may lead to improved fatigue resistance.[31] We have prepared the corresponding analogue of dye **2** (see dye **6** in the Supporting Information). However, the resulting switch was more prone to fatigue than DTE **2**, resisting only 12 cycles until 50% degradation; see the Supporting Information for the corresponding photochemical characterization.

The good water-solubility of the switches indicated their investigation in aqueous medium. Unfortunately, DTE **5** was found to be instable in neutral water. However, the DTEs **1–4** were conveniently studied in this medium (see data in Table 1). The

Table 1. Photochemical and kinetic data for the open and closed forms of DTE **1–5** and their photoswitching.

	$\lambda_{abs,open}$ [nm] ([ϵ (M^{-1} cm^{-1})])	$\lambda_{abs,closed}$ [nm] (ϵ [M^{-1} cm^{-1}])[a]	$k_{o\rightarrow c}$ [s^{-1}][b]	$k_{c\rightarrow o}$ [s^{-1}][b]	PSD (o→c)[c]	PSD (c→o)[c]	$\Phi_{o\rightarrow c}$[d]	$\Phi_{c\rightarrow o}$[e]
MeCN								
1	353 (50 900)	660 (15 800)	0.63	0.017	100% (c)	100% (o)	0.68	0.003
2	348 (30 500)	644 (17 000)	0.08	0.021	100% (c)	100% (o)	0.54	0.004
3	460 (4800)	662 (19 400)	0.0046	0.015	78% (c) 22% (o)	100% (o)	0.006	0.002
4	380 (15 700)	620 (18 700)	0.083	0.02	85% (c) 15% (o)	100% (o)	0.13	0.005
5	452 (6700)	650 (15 000)	0.0013	0.0028	44% (c) 56% (o)	100% (o)	0.001	0.001
H$_2$O								
1	356 (50 600)	661 (17 400)	1.0	0.0088	98% (c) 2% (o)	100% (o)	0.68	0.002
2	351 (33 100)	644 (18 900)	0.19	0.0096	100% (c)	100% (o)	0.41	0.003
3	466 (4900)	660 (21 700)	0.0057	0.01	60% (c) 40% (o)	100% (o)	0.004	0.002
4	382 (13 500)	616 (17 700)	0.014	0.015	80% (c) 20% (o)	100% (o)	0.02	0.004

[a] The molar absorption coefficient ϵ for the closed form is corrected for the cases of incomplete o→c conversion. [b] First-order rate constant for o→c conversion (excitation at 365 nm, monochromatic excitation source) and c→o conversion (excitation >590 nm; Xe lamp with long-pass optical filter). [c] Photostationary state distribution (PSD) determined by ^{1}H NMR spectroscopy. [d] Determined by actinometry with potassium tri-oxalatoferrate(III) trihydrate (K$_3$Fe(C$_2$O$_4$)$_3$ × 3H$_2$O); see the Supporting Information. [e] Determined by actinometry with 1,2-bis(2,4-dimethyl-5-phenyl-3-thienyl)-3,3,4,4,5,5-hexafluoro-1-cyclopentene (see the Supporting Information).
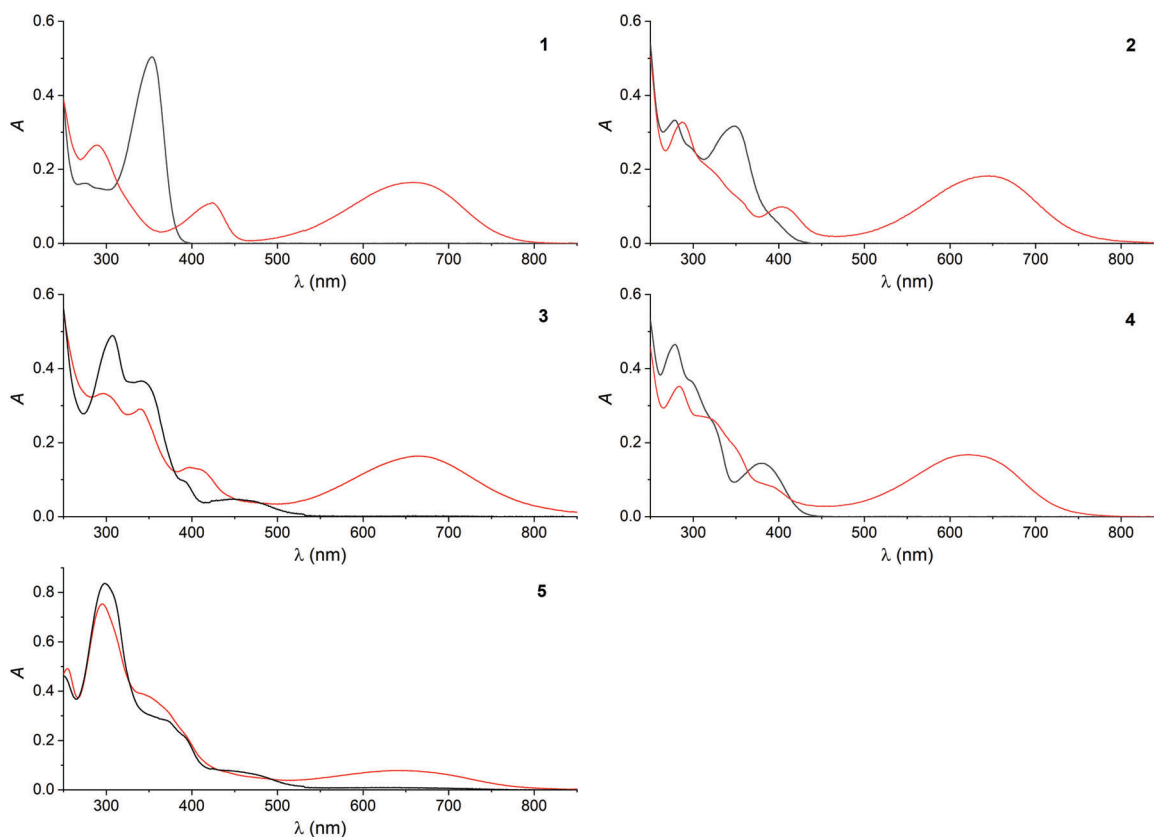

Figure 3. UV–vis absorption spectra of the DTE **1–5** in acetonitrile (10 μM for **1–4** and 7.5 μM for **5**). The black line corresponds to the open form, while the red line designates the photostationary state spectrum after irradiation with 365-nm light. In the case of **1** and **2**, the photostationary state corresponds to 100% closed form. However, for the other dyes (**3–5**) a less than quantitative conversion to the closed form is observed; see text. The long-wavelength band (λ_{max} > 600 nm) is characteristic for the closed form.

**ADVANCED
SCIENCE NEWS**

www.advancedsciencenews.com
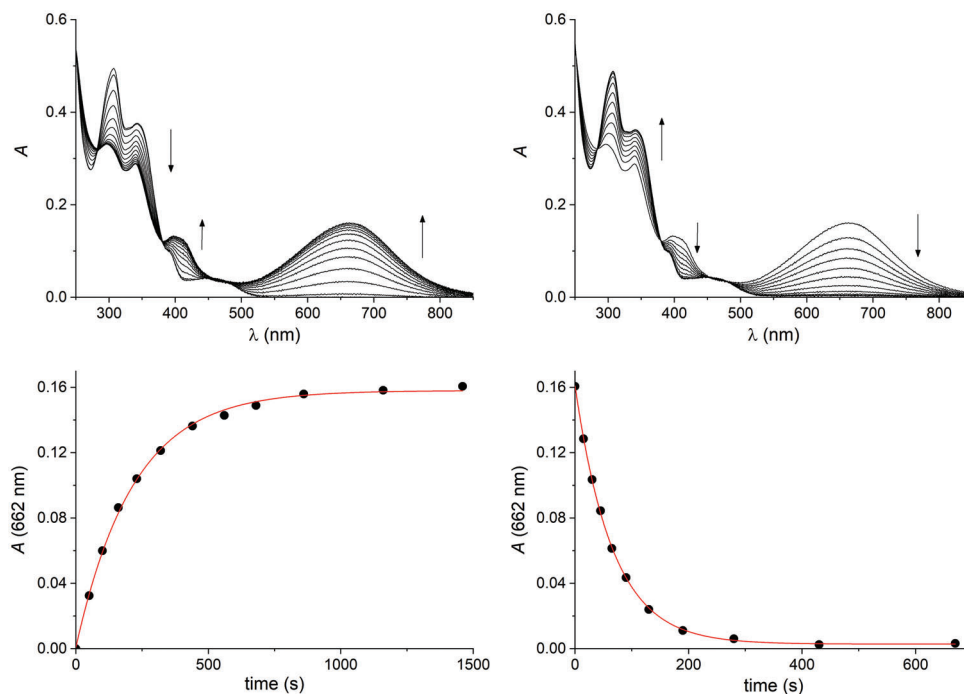
**ADVANCED
MATERIALS**

www.advmat.de

Figure 4. Irradiation spectra (top) and corresponding kinetic plots (bottom) for the ring closure (left) and ring opening (right) of DTE **3** (10 μM) in acetonitrile; see conditions in footnotes of Table 1.

long-wavelength absorption bands of the open and closed forms were not significantly altered (maximum ± 6 nm) with respect to acetonitrile as solvent. The PSD was very similar to acetonitrile, with the largest deviation observed for DTE **3**, which showed now a 60/40 c/o-distribution for irradiation at 365 nm. The ring-closing quantum yields remained reasonably high for DTE **1** ($\Phi_{o \to c}$ = 0.68) and **2** ($\Phi_{o \to c}$ = 0.41), but were rather low for **3** and **4**. Repeated switching of the DTEs (**1**–**4**) in water is possible. However, except for **1**, they show a more pronounced tendency for fatigue than in organic solvent. This is most obvious for the

DTE dyes **3** and **4** (ca. 20–40% decomposition in the course of five switching cycles). It may be argued that a background nucleophilic attack of water may involve. However, the instability of DTE **3**, for example, also maintains in acidic medium at pH 4.

2.3. Fluorescence Properties

For the investigated set of DTEs with aza-aromatic cationic moieties (**1**–**5**), we observed spectrally variable fluorescence emission for the open forms in acetonitrile (see **Figure 6**). The symmetrically substituted **1** with pyridinium arms showed a relatively weak
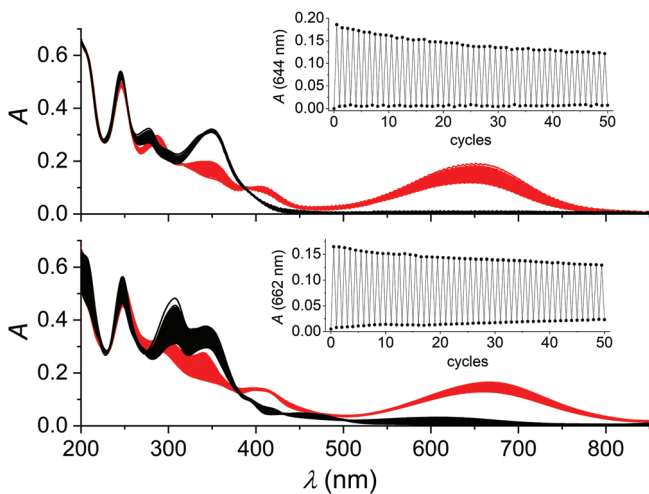

Figure 5. Switching cycles of the DTE dyes **2** (top) and **3** (bottom) in aerated acetonitrile; concentration 10 μM.
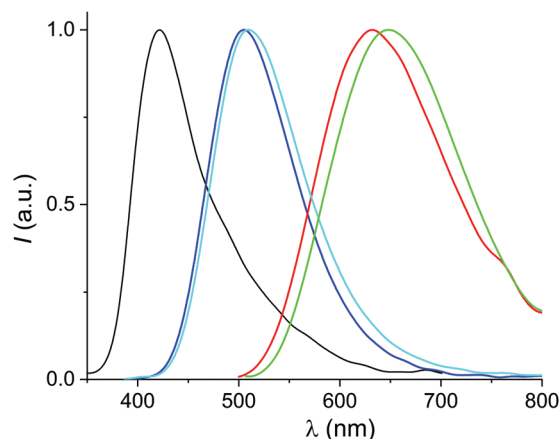

Figure 6. Normalized fluorescence spectra of the open forms of the DTE dyes **1**–**5** (10 μM) in acetonitrile. Color code: black-**1**; blue-**2**; red-**3**; cyan-**4**; green-**5**.

2300536 (6 of 11)

Table 2. Fluorescence properties of the DTE **1–5** in acetonitrile and water.

	MeCN			H$_2$O		
	$\lambda_{f,open}$ [nm][a]	Φ_f[b]	τ_f [ns][c]	$\lambda_{f,open}$ [nm][a]	Φ_f[b]	τ_f [ns][c]
1	422	0.007	0.68 (90%); 2.42 (10%)	421	0.002	0.12
2	504	0.15	5.74	509	0.13	5.46
3	632	0.02	7.49	610	0.02	1.34 (93%); 5.17 (7%)
4	509	0.03	1.92 (95%); 4.32 (5%)	508	0.004	0.37 (94%); 4.88 (6%)
5	646	<0.002	1.38 (72%); 5.02 (28%)	nd	nd	nd

[a] Maximum of fluorescence spectrum. [b] Fluorescence quantum yield; measured with quinine sulfate as standard. [c] Fluorescence lifetime, measured by time-correlated single-photon-counting. In parentheses the relative weight of each lifetime component is given, when multi-exponential decay was observed. nd: not determined due to low solubility and low stability of **5** in water.

emission with the most blue-shifted maximum (422 nm) among the herein investigated dyes. Substituting one of the pyridinium arms in **1** by a quinolinium or acridinium moiety leads to **2** and **3**. In accordance with the increased π-conjugation these derivatives feature red-shifted emission spectra with maxima at 504 and 632 nm, respectively. On substituting the pyridinium moiety in **2** and **3** with the corresponding aza-aromatic cation, the symmetric DTE switches **4** and **5** are obtained. This has some additional contribution to the red-shift of the fluorescence spectrum, but is far from being additive. The comparison of the fluorescence maxima and band shapes of **2** and **4** as well as **3** and **5** confirms that the spectral emission properties are mainly ruled by the more conjugated heteroaromatic arm (see **Table 2** and Figure 6); see also theoretical calculations below.

In order to exclude that the emission of the open form of the DTEs originates simply from the heteroaromatic cation, without implying electronic integration with the DTE core, the emission spectra of the symmetrically substituted **4** and **5** were compared with the reported data for *N*-methylquinolinium (**Quin**$^+$) and *N*-methylacridinium (**Acr**$^+$) dyes, respectively. In acetonitrile **Quin**$^+$ emits with a maximum at ≈405 nm,[59] while **Acr**$^+$ shows its maximum fluorescence at ≈495 nm.[60] These emissions are significantly blueshifted (by ca. 100–150 nm) with respect to the fluorescence spectra that were observed for the corresponding DTE dyes **4** and **5**. This points to the interpretation that the union of the heteroaromatic cation and DTE core results in a "super"-chromophore with completely altered fluorescence properties; a view that is also sustained by theoretical calculations (see below).

As regarded the emission quantum yields in acetonitrile, the highest value is observed for **2** ($\Phi_f = 0.15$). The quantum yield for **3** ($\Phi_f = 0.02$) is smaller, but still significant for a dye emitting in the red spectral region. The reason for the sharp difference between **2** and **3** seems to be a one-order-of-magnitude smaller radiative rate constant k_f for the latter (2.6×10^7 s^{-1} vs 2.7×10^6 s^{-1} for **2** and **3**, respectively). However, the non-radiative rate constant k_{nr} is very comparable for both switches [$(1.3–1.5) \times 10^8$ s^{-1}]. Notoriously, the asymmetrically substituted DTEs **2** and **3** are 5–10 times more fluorescent than their symmetric counterparts **4** and **5**, respectively. In water solution, the general trends that were observed for acetonitrile solution are confirmed for the open forms of the DTE switches **1–4**.

The closed forms of the switches do not show observable fluorescence. Eventual residual fluorescence after ring-closing of the open forms is traced back to the presence of the latter in the photostationary state (see Table 1). The lack of observation of fluorescence from the closed form is tentatively attributed to the much higher degree of π-conjugation and therefore energetically very low-lying emissive levels. These tend to deactivate preferentially through non-radiative pathways, according to the energy-gap law. Indeed, theoretical calculations (see below) predict emission in the near-infrared region at wavelengths longer than 1200 nm. As a result, the fluorescence can switched OFF and ON for repeated irradiation sequences of UV and vis light. This was clearly observed for the DTEs **2**, **3**, and **4**; see **Figure 7** for the dyes **2** and **3** and the Supporting Information for dye **4**.

2.4. Theoretical Calculations

To gain further insights into the photophysical properties of the investigated DTE switches, density-functional-theory (DFT), and time-dependent density functional theory (TD-DFT) calculations were performed. Acetonitrile as solvent was taken into account by means of the polarizable continuum model (PCM).[61] The absorption and emission energies were calculated by employing
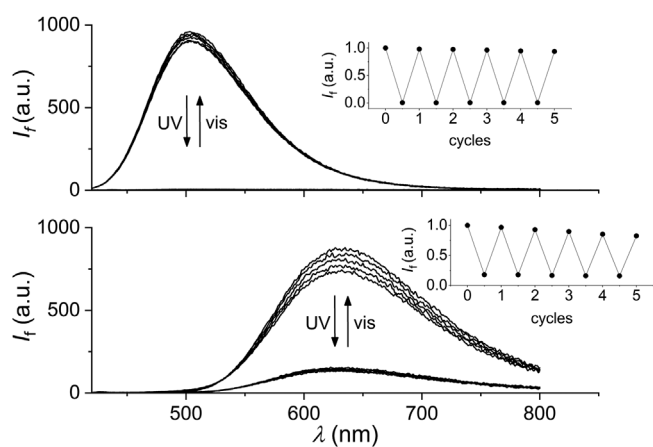

Figure 7. Repeated fluorescence switching of the DTE dyes **2** (top) and **3** (bottom) in acetonitrile; concentration 10 μM. The insets show the corresponding variations of emission intensity at the fluorescence maximum. Note that the residual fluorescence on irradiation of DTE **3o** with UV light is due to the presence of **3o** in the photostationary state.

**ADVANCED
SCIENCE NEWS**

www.advancedsciencenews.com

**ADVANCED
MATERIALS**

www.advmat.de

Table 3. TD-DFT calculated absorption and emission data for the DTE dyes **1–5**.

	Transition (f)[a]	Dominant components ([%])	E_{calc} [eV] (λ [nm])	E_{exp} [eV] (λ [nm])
		Absorption		
1o	$S_1 \leftarrow S_0$ (1.783)	LUMO←HOMO (61)	3.66 (338)	3.51 (353)
		LUMO+1←HOMO−1 (33)		
1c	$S_1 \leftarrow S_0$ (0.579)	LUMO←HOMO (94)	1.99 (624)	1.88 (660)
2o	$S_1 \leftarrow S_0$ (0.408)	LUMO←HOMO (77)	3.53 (352)	3.56 (348)
		LUMO←HOMO−1 (15)		
2c	$S_1 \leftarrow S_0$ (0.625)	LUMO←HOMO (93)	2.02 (613)	1.93 (644)
3o	$S_1 \leftarrow S_0$ (0.221)	LUMO←HOMO (83)	2.99 (415)	2.70 (460)
3c	$S_1 \leftarrow S_0$ (0.681)	LUMO←HOMO (74)	2.01 (618)	1.87 (662)
		LUMO+1←HOMO (18)		
4o	$S_1 \leftarrow S_0$ (0.350)	LUMO←HOMO (49)	3.51 (353)	3.26 (380)
		LUMO+1←HOMO−1 (39)		
4c	$S_1 \leftarrow S_0$ (0.651)	LUMO←HOMO (84)	2.18 (568)	2.00 (620)
5o	$S_1 \leftarrow S_0$ (0.084)	LUMO←HOMO (43)	2.99 (415)	2.74 (452)
		LUMO+1←HOMO−1 (40)		
5c	$S_1 \leftarrow S_0$ (0.745)	LUMO←HOMO (53)	2.13 (581)	1.91 (650)
		LUMO+2←HOMO (42)		
		Emission		
1o	$S_1 \rightarrow S_0$ (1.210)	LUMO→HOMO (96)	3.06 (405)	2.95 (420)
1c	$S_1 \rightarrow S_0$ (0.495)	LUMO→HOMO (100)	0.89 (1396)	–
2o	$S_1 \rightarrow S_0$ (0.339)	LUMO→HOMO (99)	2.58 (481)	2.46 (504)
2c	$S_1 \rightarrow S_0$ (0.560)	LUMO→HOMO (100)	0.96 (1297)	–
3o	$S_1 \rightarrow S_0$ (0.243)	LUMO→HOMO (99)	2.07 (598)	1.96 (633)
3c	$S_1 \rightarrow S_0$ (0.606)	LUMO→HOMO (100)	0.94 (1326)	–
4o	$S_1 \rightarrow S_0$ (0.311)	LUMO→HOMO (98)	2.55 (486)	2.43 (510)
4c	$S_1 \rightarrow S_0$ (0.661)	LUMO→HOMO (100)	1.06 (1172)	–
5o	$S_1 \rightarrow S_0$ (0.234)	LUMO→HOMO (98)	2.04 (607)	1.92 (645)
5c	$S_1 \rightarrow S_0$ (0.774)	LUMO→HOMO (100)	0.99 (1251)	–

[a] Oscillator strength f.

the CAM-B3LYP[62] and PBE0 functional,[63,64] respectively. These functionals have been used frequently in the literature to reproduce the experimental transition energies for DTE switches.[65–68] In all cases, the 6–311+G(2d,p) basis set was used. The comparison between experimental and theoretical absorption and emission energies is summarized in **Table 3**. The CAM-B3LYP functional has been proven to be effective for the prediction of absorption energies and the differences between the calculated and experimental values were within the accepted error limits in all cases, i.e., differences <0.3 eV. However, the precision of CAM-B3LYP is drastically reduced for the calculation of the emission spectra (see the Supporting Information), a fact that has been noted previously for other chromophores as well.[69] Therefore, we employed the PBE0 functional, which stood out in a benchmarking test (see the Supporting Information). This allowed us to reproduce the experimental emission energies with good accuracy (differences of 0.10–0.12 eV). Especially of interest is the fact that the open forms are predicted to show fluorescence in the visible spectral range (400–650 nm, depending on the degree of conjugation of the heteroaromatic cationic moieties), which is in concordance with the experimental observations. In contrast, the much more conjugated closed form is predicted to emit in the near-infrared spectral range (1170–1400 nm). In practical terms, due to the energy-gap law, such emissions are expected to be very weak, if at all observable.

For the ring-open isomers the $S_1 \leftarrow S_0$ transition, ascribed to the long-wavelength absorption band, implies mainly the HOMO and LUMO (Table 3) and these molecular frontier orbitals are located over the more conjugated arm of the asymmetrically substituted DTE dyes **2** and **3**. For the symmetrically substituted DTE dyes **1**, **4**, and **5** in addition to the HOMO and LUMO also a significant contribution of the HOMO−1 and LUMO+1 was noted and the implied molecular orbitals are located over the two cationic moieties of the dyes. For the latter molecules, it is interesting to note that due to their apparent C_2 symmetry the LUMO and LUMO+1 are nearly degenerate.

The $S_1 \leftarrow S_0$ transition, ascribed to the long-wavelength absorption band of the ring-closed DTEs, implies also principally the HOMO and LUMO (see Table 3). The HOMO is situated over the central DTE unit, involving the perfluorocyclopentene and the two thiophene rings, while the LUMO is spread out over the complete molecule. The $S_1 \rightarrow S_0$ emission, either of the open or the closed form (not visible in the latter case), is entirely characterized by the LUMO→HOMO transition.

2300536 (8 of 11)

**ADVANCED
SCIENCE NEWS**

www.advancedsciencenews.com
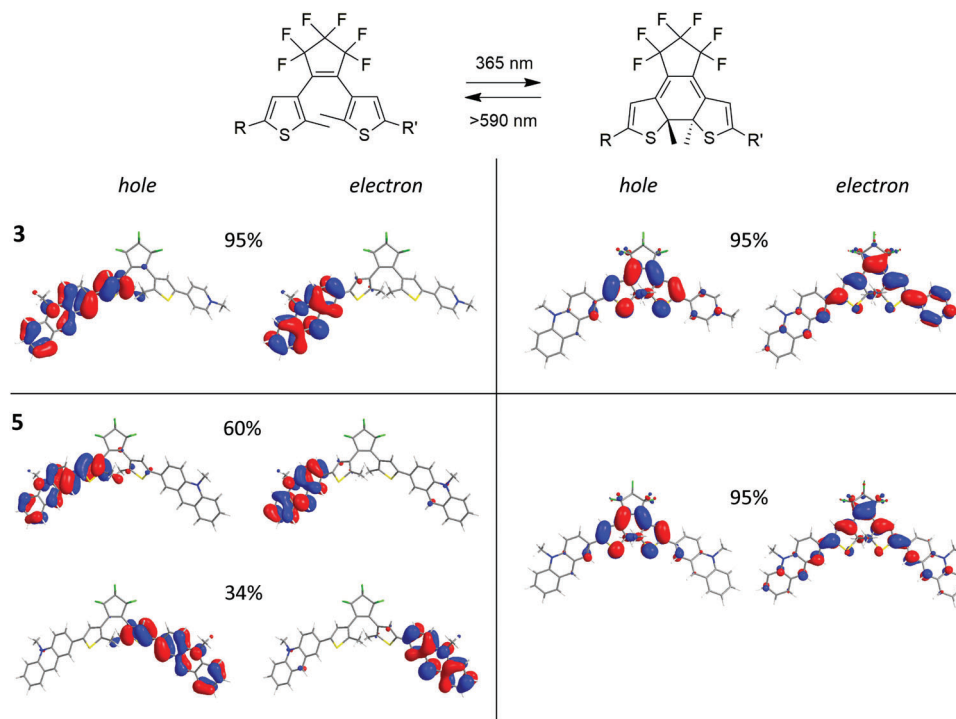
**ADVANCED
MATERIALS**

www.advmat.de

Figure 8. Natural transition orbital analysis (NTO) for the $S_1 \leftarrow S_0$ transition of the open (left) and closed (right) forms of DTE **3** (top) and **5** (bottom).

When several frontier molecular orbitals are involved in a transition, natural transition orbitals (NTOs) are an adequate tool for visualizing the involved transitions.[70] From the NTO analysis of the $S_1 \leftarrow S_0$ transition of the open forms of DTEs, two distinct patterns can be distinguished, one for asymmetrically substituted and the other for symmetrically substituted DTEs. In the asymmetric ones (see **Figure 8** for **3o** and the Supporting Information for the other DTEs) the hole is located over the moiety with the higher conjugated aza-heteroaromatic (quinolinium for **2o** or acridinium for **3o**), including the thiophene moiety of the DTE core. However, the electron is located only over the cationic moiety of the same arm. For the symmetrically substituted DTEs **4** and **5** the hole and the electron have two components (see Figure 8 for **5o**), one for each of the cationic arms. In both components, the hole is centered over the thiophene and aza-heteroaromatic moiety of one of the arms, while the electron is exclusively located over the aza-heteroaromatic cation. In the case of **1** the hole is found over the thiophenes of both arms for the two components and the electron is mainly situated over the pyridinium moieties of both arms.

For the closed forms of the dyes only one component is found in the NTO analysis of the $S_1 \leftarrow S_0$ transition (see Figure 8 and the Supporting Information). For all dyes, the hole is placed over the DTE nucleus (the perfluorocyclopentene ring and the two thiophene rings), while the electron is distributed across the entire molecule including both arms for the symmetrically substituted DTE dyes, e.g., **5** in Figure 8. For the unsymmetrically substituted dyes (e.g., **3** in Figure 8), the electron is mainly found on the pyridinium branch.

3. Conclusion

The photochemical and photophysical properties of DTEs with appended heteroaromatic cationic moieties can be fine-tuned by the degree of π-conjugation. The photoswitching properties were found to be comparable to other DTEs, except when acridinium units were involved. In the latter cases the ring-closing efficiency is drastically diminished. This is tentatively assigned to the occurrence of charge-transfer phenomena as competitive excited-state processes. Interestingly, the switches in their open form show fluorescence emission in the visible spectral range (400–650 nm), which is dependent on the extent of π-conjugation of the heteroaromatic unit. The most red-shifted emission maxima are seen for the DTE-acridinium switches (**3** and **5**). No fluorescence in the inspected spectral range until 900 nm was observed for the closed forms. DFT calculations predict that emissions of the closed forms would be occurring in the near-infrared spectral range above ca. 1200 nm. This is in accordance with an energetically very low-lying emissive state due to the highly conjugated nature of the closed form. The observation of fluorescence from plain DTE switches is very rare. The herein described series of compounds and their detailed study open interesting perspectives for their application in information processing, data storage, imaging, or sensing.

4. Experimental Section

All details about the synthesis, the analytical characterization of the compounds, crystal data, the photochemical experiments, and the theoretical calculations can be found in the Supporting Information.

2300536 (9 of 11)

Supporting Information

Acknowledgements

Conflict of Interest

The authors declare no conflict of interest.

Data Availability Statement

Research data are not shared.

Keywords

[1] B. L. Feringa, W. R. Browne, *Molecular Switches, 2 Volume Set*, John Wiley & Sons, New York, USA **2011**.

[2] A. Goulet-Hanssens, F. Eisenreich, S. Hecht, *Adv. Mater.* **2020**, *32*, 1905966.

[3] M.-M. Russew, S. Hecht, *Adv. Mater.* **2010**, *22*, 3348.

[4] J. Volarić, W. Szymanski, N. A. Simeth, B. L. Feringa, *Chem. Soc. Rev.* **2021**, *50*, 12377.

[5] M. Berberich, A.-M. Krause, M. Orlandi, F. Scandola, F. Würthner, *Angew. Chem., Int. Ed.* **2008**, *47*, 6616.

[6] J. Andréasson, U. Pischel, *Chem. Soc. Rev.* **2010**, *39*, 174.

[7] J. Andréasson, U. Pischel, *Chem. Soc. Rev.* **2015**, *44*, 1053.

[8] J. Andréasson, U. Pischel, S. D. Straight, T. A. Moore, A. L. Moore, D. Gust, *J. Am. Chem. Soc.* **2011**, *133*, 11641.

[9] M. Bälter, S. Li, J. R. Nilsson, J. Andréasson, U. Pischel, *J. Am. Chem. Soc.* **2013**, *135*, 10230.

[10] D. Gust, J. Andréasson, U. Pischel, T. A. Moore, A. L. Moore, *Chem. Commun.* **2012**, *48*, 1947.

[11] A. E. Keirstead, J. W. Bridgewater, Y. Terazono, G. Kodis, S. Straight, P. A. Liddell, A. L. Moore, T. A. Moore, D. Gust, *J. Am. Chem. Soc.* **2010**, *132*, 6588.

[12] T. B. Norsten, N. R. Branda, *Adv. Mater.* **2001**, *13*, 347.

[13] P. Remón, D. González, S. M. Li, N. Basílio, J. Andréasson, U. Pischel, *Chem. Commun.* **2019**, *55*, 4335.

[14] M. J. Fuchter, *J. Med. Chem.* **2020**, *63*, 11436.

[15] K. Hüll, J. Morstein, D. Trauner, *Chem. Rev.* **2018**, *118*, 10710.

[16] W. A. Velema, W. Szymanski, B. L. Feringa, *J. Am. Chem. Soc.* **2014**, *136*, 2178.

[17] R. S. Stoll, S. Hecht, *Angew. Chem., Int. Ed.* **2010**, *49*, 5054.

[18] D.-H. Qu, Q.-C. Wang, Q.-W. Zhang, X. Ma, H. Tian, *Chem. Rev.* **2015**, *115*, 7543.

[19] P. Ferreira, B. Ventura, A. Barbieri, J. P. Da Silva, C. A. T. Laia, A. J. Parola, N. Basílio, *Chem. - Eur. J.* **2019**, *25*, 3477.

[20] P. Máximo, M. Colaço, S. R. Pauleta, P. J. Costa, U. Pischel, A. J. Parola, N. Basílio, *Org. Chem. Front.* **2022**, *9*, 4238.

[21] O. Nevskyi, D. Sysoiev, A. Oppermann, T. Huhn, D. Wöll, *Angew. Chem., Int. Ed.* **2016**, *55*, 12698.

[22] M. Bossi, V. Belov, S. Polyakova, S. W. Hell, *Angew. Chem., Int. Ed.* **2006**, *45*, 7462.

[23] D. Kim, A. Aktalay, N. Jensen, K. Uno, M. L. Bossi, V. N. Belov, S. W. Hell, *J. Am. Chem. Soc.* **2022**, *144*, 14235.

[24] K. Uno, M. L. Bossi, M. Irie, V. N. Belov, S. W. Hell, *J. Am. Chem. Soc.* **2019**, *141*, 16471.

[25] M. Irie, M. Mohri, *J. Org. Chem.* **1988**, *53*, 803.

[26] S. Nakamura, M. Irie, *J. Org. Chem.* **1988**, *53*, 6136.

[27] H.-B. Cheng, S. Zhang, E. Bai, X. Cao, J. Wang, J. Qi, J. Liu, J. Zhao, L. Zhang, J. Yoon, *Adv. Mater.* **2022**, *34*, 2108289.

[28] M. Irie, T. Fukaminato, K. Matsuda, S. Kobatake, *Chem. Rev.* **2014**, *114*, 12174.

[29] J. Zhang, H. Tian, *Adv. Opt. Mater.* **2018**, *6*, 1701278.

[30] M. Irie, *Chem. Rev.* **2000**, *100*, 1685.

[31] M. Herder, B. M. Schmidt, L. Grubert, M. Pätzel, J. Schwarz, S. Hecht, *J. Am. Chem. Soc.* **2015**, *137*, 2738.

[32] I. Cheng-Yi Hou, F. Berger, A. Narita, K. Müllen, S. Hecht, *Angew. Chem., Int. Ed.* **2020**, *59*, 18532.

[33] S. Fredrich, R. Göstl, M. Herder, L. Grubert, S. Hecht, *Angew. Chem., Int. Ed.* **2015**, *55*, 1208.

[34] Z. Zhang, W. Wang, M. O'Hagan, J. Dai, J. Zhang, H. Tian, *Angew. Chem., Int. Ed.* **2022**, *61*, e202205758.

[35] S. Saita, T. Yamaguchi, T. Kawai, M. Irie, *ChemPhysChem* **2005**, *6*, 2300.

[36] M. Shigeiwa, S. Maeda, H. Gorohmaru, S. Imamura, M. Irie, *Mol. Cryst. Liq. Cryst.* **2005**, *430*, 173.

[37] K. Mori, Y. Ishibashi, H. Matsuda, S. Ito, Y. Nagasawa, H. Nakagawa, K. Uchida, S. Yokojima, S. Nakamura, M. Irie, H. Miyasaka, *J. Am. Chem. Soc.* **2011**, *133*, 2621.

[38] C. Benitez-Martin, S. Li, A. Dominguez-Alfaro, F. Najera, E. Pérez-Inestrosa, U. Pischel, J. Andréasson, *J. Am. Chem. Soc.* **2020**, *142*, 14854.

[39] C. Yun, J. You, J. Kim, J. Huh, E. Kim, *J. Photochem. Photobiol., C* **2009**, *10*, 111.

[40] K. Shibata, L. Kuroki, T. Fukaminato, M. Irie, *Chem. Lett.* **2008**, *37*, 832.

[41] J. Piard, R. Métivier, M. Giraud, A. Léaustic, P. Yu, K. Nakatani, *New J. Chem.* **2009**, *33*, 1420.

[42] H.-H. Liu, Y. Chen, *J. Phys. Chem. A* **2009**, *113*, 5550.

[43] Z. Xu, Q. T. Liu, X. Wang, Q. Liu, D. Hean, K. C. Chou, M. O. Wolf, *Chem. Sci.* **2020**, *11*, 2729.

[44] Y.-C. Jeong, S. I. Yang, K.-H. Ahn, E. Kim, *Chem. Commun.* **2005**, 2503.

[45] K. Uno, H. Niikura, M. Morimoto, Y. Ishibashi, Miyasaka, H., M. Irie, *J. Am. Chem. Soc.* **2011**, *133*, 13558.

[46] T. Fukaminato, T. Doi, N. Tamaoki, K. Okuno, Y. Ishibashi, H. Miyasaka, M. Irie, *J. Am. Chem. Soc.* **2011**, *133*, 4984.

[47] T. Fukaminato, T. Sasaki, T. Kawai, N. Tamai, M. Irie, *J. Am. Chem. Soc.* **2004**, *126*, 14843.

[48] M. Irie, T. Fukaminato, T. Sasaki, N. Tamai, T. Kawai, *Nature* **2002**, *420*, 759.

**ADVANCED
SCIENCE NEWS**

www.advancedsciencenews.com

**ADVANCED
MATERIALS**

www.advmat.de

[49] F. M. Raymo, M. Tomasulo, *Chem. Soc. Rev.* **2005**, *34*, 327.

[50] G. Naren, W. Larsson, C. Benitez-Martin, S. Li, E. Perez-Inestrosa, B. Albinsson, J. Andreasson, *Chem. Sci.* **2021**, *12*, 7073.

[51] G. Naren, S. Li, J. Andréasson, *Chem. Commun.* **2020**, *56*, 3377.

[52] L. N. Lucas, J. J. D. de Jong, J. H. van Esch, R. M. Kellogg, B. L. Feringa, *Eur. J. Org. Chem.* **2003**, 155.

[53] K. Higashiguchi, K. Matsuda, Y. Asano, A. Murakami, S. Nakamura, M. Irie, *Eur. J. Org. Chem.* **2005**, 91.

[54] T. van Leeuwen, T. C. Pijper, J. Areephong, B. L. Feringa, W. R. Browne, N. Katsonis, *J. Mater. Chem.* **2011**, *21*, 3142.

[55] D. Ding, H. Jiang, X. Ma, J. J. Nash, H. I. Kenttämaa, *J. Org. Chem.* **2020**, *85*, 8415.

[56] However, no UV-light-induced colorization was observed for the crystals of either compound, i.e., **2** or **4**.

[57] K. Matsuda, Y. Shinkai, T. Yamaguchi, K. Nomiyama, M. Isayama, M. Irie, *Chem. Lett.* **2003**, *32*, 1178.

[58] Rehm–Weller equation: $\Delta G = E_{ox} - E_{red} - E^* + C$ (cf. D. Rehm, A. Weller, Ber. Bunsenges. Phys. Chem. 1969, 73, 834); redox potentials of model compounds: $E_{ox} = 1.46$ V (vs SCE in MeCN) for 1,2-bis(2-methyl-5-(4-methylphenyl)thien-3-yl)perfluorocyclopent-1-ene (cf. ref. 31), $E_{red} = -0.49$ V (vs SCE in MeCN) for 9-mesityl-*N*-methylacridinium (cf. N. A. Romero, D. A. Nicewicz, J. Am. Chem. Soc. 2014, 136, 17024); excitation energy of **3o**: $E^* = 2.70$ eV; Coulomb term: $C = -0.06$ eV.

[59] F. Rodríguez-Prieto, C. Costa Corbelle, B. Fernández, J. A. Pedro, M. C. Ríos Rodríguez, M. Mosquera, *Phys. Chem. Chem. Phys.* **2018**, *20*, 307.

[60] A. C. Benniston, A. Harriman, P. Li, J. P. Rostron, H. J. van Ramesdonk, M. M. Groeneveld, H. Zhang, J. W. Verhoeven, *J. Am. Chem. Soc.* **2005**, *127*, 16054.

[61] J. Tomasi, B. Mennucci, R. Cammi, *Chem. Rev.* **2005**, *105*, 2999.

[62] T. Yanai, D. P. Tew, N. C. Handy, *Chem. Phys. Lett.* **2004**, *393*, 51.

[63] C. Adamo, V. Barone, *J. Chem. Phys.* **1999**, *110*, 6158.

[64] M. Ernzerhof, G. E. Scuseria, *J. Chem. Phys.* **1999**, *110*, 5029.

[65] S. Aloïse, M. Sliwa, G. Buntinx, S. Delbaere, A. Perrier, F. Maurel, D. Jacquemin, M. Takeshita, *Phys. Chem. Chem. Phys.* **2013**, *15*, 6226.

[66] S. Aloïse, R. Yibin, I. Hamdi, G. Buntinx, A. Perrier, F. Maurel, D. Jacquemin, M. Takeshita, *Phys. Chem. Chem. Phys.* **2014**, *16*, 26762.

[67] A. Fihey, D. Jacquemin, *Chem. Sci.* **2015**, *6*, 3495.

[68] D. Jacquemin, E. A. Perpète, F. Maurel, A. Perrier, *Phys. Chem. Chem. Phys.* **2010**, *12*, 13144.

[69] A. Charaf-Eddin, A. Planchat, B. Mennucci, C. Adamo, D. Jacquemin, *J. Chem. Theory Comput.* **2013**, *9*, 2749.

[70] R. L. Martin, *J. Chem. Phys.* **2003**, *118*, 4775.